Reference: *Biol. Bull.* **201:** 154–166. (October 2001)

Ontogenetic Changes in Mantle Kinematics During Escape-Jet Locomotion in the Oval Squid, *Sepioteuthis lessoniana* Lesson, 1830

JOSEPH T. THOMPSON* AND WILLIAM M. KIER

Department of Biology, CB#3280 Coker Hall, University of North Carolina, Chapel Hill, North Carolina 27599-3280

Abstract. We investigated the kinematics of mantle movement during escape jet behavior in an ontogenetic series of *Sepioteuthis lessoniana*, the oval squid. Changes in mantle diameter during the jet were measured from digitized S-VHS video fields of tethered animals that ranged in age from hatchlings to 9 weeks. The amplitude of both mantle contraction and mantle hyperinflation (expressed as percent change from the resting mantle diameter) during an escape jet was significantly greater in hatchlings than in older, larger squid ($P < 0.05$). The maximum amplitude of mantle contraction during the escape jet decreased from an average of −40% in hatchlings to −30% in the largest animals studied. The maximum amplitude of mantle hyperinflation decreased from an average of 18% in hatchlings to 9% in the largest squid examined. In addition, the maximum rate of mantle contraction decreased significantly during ontogeny ($P < 0.05$), from a maximum of 8.6 mantle circumference lengths per second (L/s) in hatchlings to 3.8 L/s in the largest animals studied. The ontogenetic changes in the mantle kinematics of the escape jet occurred concomitantly with changes in the organization of collagenous connective tissue fiber networks in the mantle. The alteration in mantle kinematics during growth may result in proportionately greater mass flux during the escape jet in newly hatched squid than in larger animals.

Received 13 December 2000; accepted 8 May 2001.

* To whom correspondence should be addressed. E-mail: joethomp@email.unc.edu

Abbreviations: DML, dorsal mantle length; IM-1, intramuscular fiber system 1; IM-2, intramuscular fiber system 2; IM-3, intramuscular fiber system 3.

Introduction

Post-embryonic change in morphology is a common feature of most organisms (*e.g.*, Werner, 1988). Such ontogenetic modifications may affect the ecology of the organism (Calder, 1984; Werner, 1988; Stearns, 1992) and may provide insight into the evolution of form and function, yet they are often neglected in studies of functional morphology and comparative biomechanics. Significant effects on the life cycle of an organism need not involve dramatic alterations of morphology during ontogeny. For example, at hatching, cephalopod molluscs are broadly similar in form to adults (Boletzky, 1974; Sweeney *et al.*, 1992). Yet these tiny hatchlings grow several orders of magnitude in size, shift from the neuston or plankton to the benthos or nekton (Marliave, 1980; Hanlon *et al.*, 1985), and may use different mechanisms to capture prey (O'Dor *et al.*, 1985; Chen *et al.*, 1996; Kier, 1996) and to locomote (Villanueva *et al.*, 1995). In many cases, these life-cycle changes are correlated with morphological alterations that, while not always as drastic as the wholesale changes that occur during the metamorphosis of some other marine molluscs, may be equally important in their effect on the performance or ecology of the animal.

Cephalopods depend upon a hydrostatic skeleton for support during locomotion and movement. In the mantle of loliginid squid, skeletal support for locomotion is provided by a complex arrangement of fibers of muscle and of collagenous connective tissue (Ward and Wainwright, 1972; Bone *et al.*, 1981). The connective tissue fibers are arranged in five highly organized networks: the inner and outer tunics, and three distinct systems of intramuscular fibers (Ward and Wainwright, 1972; Bone *et al.*, 1981; for review, see Gosline and DeMont, 1985). These networks of colla-

gen fibers help control changes in mantle shape during contraction of the muscles that power locomotion. In addition, the intramuscular collagen fibers store elastic energy during the exhalant phase of the jet and return the energy to help restore mantle shape and refill the mantle cavity (Ward and Wainwright, 1972; Bone *et al.*, 1981; Gosline *et al.*, 1983; Gosline and Shadwick, 1983a; Shadwick and Gosline, 1985; MacGillivray *et al.*, 1999).

The organization of mantle connective tissue changes significantly during ontogeny in *Sepioteuthis lessoniana*, the oval squid. In hatchlings, the arrangement of outer tunic and intramuscular collagen fibers is hypothesized to permit large-amplitude movements of the mantle (Thompson, 2000; Thompson and Kier, 2001). In early ontogeny, the fiber angle of the collagen fiber networks changes exponentially, potentially limiting the amplitude of movement as the squid grow (Thompson, 2000; Thompson and Kier, 2001). Although these changes in connective tissue organization do not constitute a discrete metamorphosis, their influence on the mechanical properties of the mantle and the mechanics of jet locomotion may be considerable.

To explore the implications of changes in the organization of mantle connective tissue for the mechanics of jet locomotion, we studied the kinematics of the escape jet in an ontogenetic series of *S. lessoniana*. The escape jet is a distinct form of locomotion that typically involves a brief initial hyperinflation of the mantle (*i.e.*, the mantle is expanded radially beyond its resting diameter; see Gosline *et al.*, 1983) followed by a rapid contraction that expels water from the mantle cavity *via* the muscular funnel. In tethered *S. lessoniana*, we measured ontogenetic changes in the following kinematic parameters during the escape jet: the amplitude of mantle hyperinflation and mantle contraction, the rate of mantle contraction, and the frequency of escape jetting. In addition, we used measurements of mantle radius, mantle wall thickness, and mantle cavity volume to calculate the relative mass flux produced during the escape jet. Finally, we examined the relationship between mantle connective tissue morphology and mantle kinematics during the escape jet.

Materials and Methods

Animals

We obtained an ontogenetic series of *Sepioteuthis lessoniana* Lesson, 1830. We chose *S. lessoniana* for the experiments because members of this species hatch at a large size relative to other squid (5–7 mm dorsal mantle length and 0.01–0.03 g body weight) and, like other squid in the family Loliginidae, they are capable of escape-jet locomotion immediately upon hatching (Fields, 1965; Choe, 1966; Packard, 1969; Moynihan and Rodaniche, 1982; Segawa, 1987; Gilly *et al.*, 1991).

We used *S. lessoniana* embryos that were collected from three locations (Gulf of Thailand; Okinawa Island, Japan; Tokyo Region, East Central Japan) over a 2-year period and reared (Lee *et al.*, 1994) by the National Resource Center for Cephalopods (NRCC) at the University of Texas Medical Branch (Galveston, TX). Each of the three cohorts consisted of thousands of embryos from six to eight different egg mops. Thus, it is likely that the sample populations were not the offspring of a few closely related individuals, but were representative of the natural population at each collection site.

Commencing at hatching, and at weekly intervals thereafter, live squid were sent *via* overnight express shipping from the NRCC to the University of North Carolina. Animals from each of the following eight age classes were used in the experiments: newly hatched and 1, 2, 3, 4, 5, 6, and 9 weeks after hatching. These age classes correspond to the early life history stages defined by Segawa (1987), in which the squid achieve external adult morphology at a dorsal mantle length (DML) of about 40 mm (age ~6 week) and begin to mature sexually at 150 mm DML (age >9 weeks).

Prior to the start of the experiments, the animals were allowed about 30 min to equilibrate in an 80-l circular holding tank. The temperature (23 °C) and salinity (35 ppt) of the water in the holding tanks matched the temperature and salinity of the water in which the squid were raised. Circular water flow in the tank helped keep the squid swimming parallel to the sides of the tank to prevent injury. There were never more than seven squid in the holding tank at one time, and the maximum time an individual spent in the tank was 4 h.

Tethering

Initially, we attempted to measure mantle kinematics in free-swimming squid. The small size of the hatchling squid, combined with their inability to maintain position in flow, made it difficult to videotape at high magnification and thus obtain adequate spatial resolution for the kinematic measurements. To allow videotaping at high magnification and to increase the spatial resolution of the edges of the mantle, and thus the accuracy of the kinematic measurements, the squid were tethered.

Individual squid were removed from the holding tank with a glass beaker and anesthetized lightly in a 1:1 solution of 7.5% $MgCl_2$: artificial seawater (Messenger *et al.*, 1985). Anesthesia durations varied with the size of the animal (longer times for larger animals) but were never longer than 2 min. While anesthetized, the squid were tethered (Fig. 1). A needle (0.3-mm-diameter insect pin for smaller animals or 0.7-mm-diameter hypodermic needle for larger animals) was inserted through the brachial web of the squid, anterior to the brain cartilage and posterior to the buccal mass. The needle was positioned between these two rigid structures to prevent it from tearing the soft tissue of the squid. The

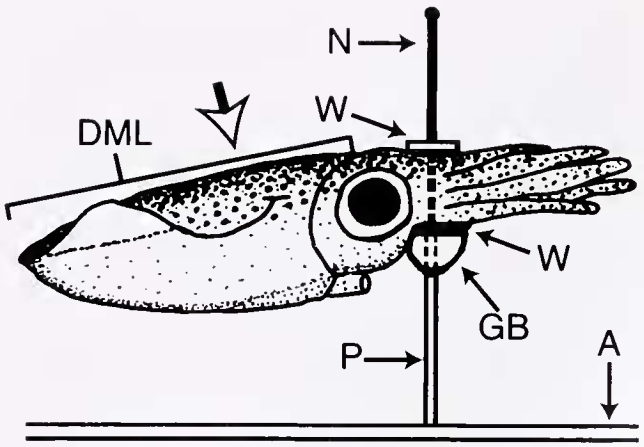

Figure 1. The tethering apparatus. A, acrylic plastic base; GB, glue bead; N, needle; P, post; W, plastic washer. DML indicates dorsal mantle length; white arrow points at ⅓ DML.

needle was inserted into a hollow stainless steel post (hypodermic tubing) attached to a sheet of acrylic plastic. The needle fit tightly in the hollow post to prevent movement. Flat, polyethylene washers on the post and needle were positioned above and below the head to prevent vertical movement.

Insertion of the needle through the anesthetized squid was rapid and required minimal handling of the animal. Individuals of this species become nearly transparent under anesthesia, making the buccal mass and the brain cartilage readily visible. Needle placement was verified after the experiment by examination of the location of the needle entrance and exit wounds.

Tethered squid were transferred to the video arena (0.4 m long by 0.2 m wide by 0.15 m deep) filled with aerated 23 °C artificial seawater and were allowed to recover. Tethered squid remained alive and in apparent good health for up to several hours, though most squid were tethered for fewer than 15 min.

Critique of tethering

Although tethering is an invasive technique, there were several indications that it was not unduly traumatic to the squid. First, tethered squid behaved similarly to the animals in the holding tank. Both the tethered and free-swimming squid spent most of the time hovering using the fins and low-amplitude jets. Second, unlike squid that are in distress or startled, more than 90% of the tethered animals did not eject ink. Third, the chromatophore patterns of tethered squid did not differ qualitatively from the patterns exhibited by the free-swimming squid in the holding tank. Finally, squid that were untethered and returned to the holding tank swam normally and could survive for several hours. It is not known how long these animals could have survived, because all the animals were killed for histological analysis after the day's experiments were completed.

Tethering did, however, affect two aspects of swimming behavior. Tethered squid (1) performed escape jets with higher frequency and (2) performed more consecutive escape jets than the free-swimming squid in the holding tank. It is possible that the tethering apparatus may have affected mantle kinematics by restricting the flow of water out of the funnel. This is unlikely because the post was between 30% and 50% of the minimum funnel aperture in hatchlings and less than 20% of the minimum funnel diameter in the largest animals studied. In addition, the tethering apparatus did not contact the funnel during the experiments.

Mantle kinematics

Escape-jet behavior was recorded from above with a Panasonic AG-450 S-VHS professional video camera. The camera was adjusted so that the squid filled as much of the field of view as possible. To maximize the measurement resolution, the animal was oriented with the long axis of the mantle vertical in the video field (*i.e.*, perpendicular to the video scan lines). Though the animals were free to rotate around the tether during the experiments, most remained near the original orientation. The frame rate of the camera (60 video fields per second) was more than 10 times faster than the observed frequency of the mantle jetting cycle. To reduce image blur, the high-speed shutter of the camera was set at 1/1000 s. Illumination was adjusted by means of a variac to the minimum level necessary to provide good contrast between the squid and the background.

Videotapes were analyzed using a Panasonic AG-1980P professional S-VHS videocassette recorder to identify escape-jet sequences suitable for digitizing. Only those sequences in which the mantle remained in the same orientation (*i.e.*, the mantle remained nearly horizontal and did not twist relative to the head) were digitized. Individual video fields were digitized using an Imagenation (Beaverton, OR) PXC200 frame-grabber card in a microcomputer.

Mantle diameter changes during vigorous escape jets were measured from digitized video fields using morphometrics software (SigmaScan Pro 4.0, SPSS Science, Chicago, IL). Diameter at ⅓ of the dorsal mantle length (DML) was measured in each video field prior to the start of and throughout the duration of an escape jet. The mantle diameter at ⅓ DML (from dorsal mantle edge, Fig. 1) was selected because the greatest amplitude mantle movements occurred at that location in all squid examined. We normalized the data by dividing the mantle diameter measured in each video field by the resting diameter (=diameter of the anesthetized squid at ⅓ DML) of the squid. Normalization by the resting mantle diameter standardized the analysis of mantle hyperinflation and mantle contraction data among the squid and allowed for comparisons between animals of

different size. More than five escape-jet sequences were analyzed from each animal. Only the sequences that yielded the greatest mantle hyperinflation and the greatest mantle contraction were reported.

For many of the escape-jet sequences, the mantle diameter data were plotted against time. Time was estimated from the video camera frame rate (approximately 0.017 s per video field). To correct for differences in animal size, the diameter change between consecutive video fields was divided by the resting mantle diameter. The rate of mantle contraction was determined by dividing the mantle diameter change between successive video fields by 0.017 s. This calculation yielded a set of incremental rates of mantle contraction. The highest incremental rate was reported as the maximum rate of mantle contraction for that animal.

The frequency of escape jets was calculated by dividing the number of complete escape-jet cycles (the exhalant plus the inhalant phases) by the time required to perform the behavior. Time was estimated from the frame rate of the video camera as above. Measurements were made only from video sequences of squid that performed two or more escape jets in rapid succession. Multiple measurements were made for each squid, but only the highest calculated escape-jet frequency was reported.

Morphometrics

The dorsal mantle length of anesthetized squid was measured to the nearest 0.1 mm using calipers. We chose dorsal mantle length as a measure of squid size because it is simple to measure accurately and it correlates strongly with squid wet weight (Segawa, 1987).

The volume of the mantle cavity was measured for most animals after videotaping. Each squid was anesthetized (Messenger *et al.*, 1985) at 20 °C for 15 min to relax the mantle musculature. The animal was then lifted from the anesthetic by the arms so that the mantle cavity remained filled with water. The exterior of the squid was gently blotted dry and the animal weighed on an electronic balance to the nearest 0.0001 g. The squid was returned to the water and then lifted by the tip of the mantle so that water emptied from the mantle cavity. The mantle was squeezed gently, in the posterior to anterior direction, to aid draining of the mantle cavity. The outside of the squid was blotted dry and the animal weighed again. We calculated the volume of the mantle cavity by dividing the difference in weight between the two measurements by the density of seawater at 20 °C (1.024×10^3 kg m^{-3}). This procedure was repeated three to five times for each squid, and the average mantle cavity volume was recorded. We normalized the volume measurements by dividing the mantle cavity volume by the wet weight of the squid.

Mantle radius was measured in all the squid. Resting mantle diameter was measured from digitized video frames of the dorsal mantle of anesthetized animals. The mantle was assumed to be cylindrical, and the diameter was measured at ⅓ DML. Mantle radius was then calculated from the diameter data.

The thickness of the mantle wall was measured in 21 specimens. Anesthetized animals were decapitated and a transverse slice of the mantle was made at one-third DML. A digital image of the slice was captured using a dissecting microscope, and the thickness of the mantle wall at the ventral midline was measured using morphometrics software.

The mantle wall thickness and radius were used to calculate mantle circumferential strain during the escape jet. The circumferential strain experienced during jet locomotion at the midpoint in the thickness of the mantle wall was calculated using the following equation from MacGillivray *et al.* (1999):

$$\epsilon_c = 1 - [(R_f - \tfrac{1}{2} t_f)/(R_i - \tfrac{1}{2} t_i)] \quad (1)$$

ϵ_c is the circumferential strain, R_i is the initial ("resting") outer radius of the mantle, R_f is the final outer radius of the contracted mantle, t_i is the initial thickness of the mantle wall, and t_f is the thickness of the contracted mantle wall. The resting outer radius and mantle wall thickness, R_i and t_i, were measured from the digital images. The final outer radius of the contracted mantle, R_f, was measured from the videotapes, and t_f was then calculated using the following equation from MacGillivray *et al.* (1999):

$$t_f = R_f - [R_f^2 - t_i(2R_i - t_i)]^{0.5} \quad (2)$$

By convention, negative circumferential strain values indicate contraction of the mantle, and positive values indicate hyperinflation of the mantle.

Statistics

All correlations were made using the Spearman rank order correlation (Sokal and Rohlf, 1981). This nonparametric statistical test was used because the data for dorsal mantle length were not distributed normally (Kolmogorov-Smirnov goodness of fit test, $P < 0.01$; Zar, 1996) due to a sample bias toward smaller squid.

The mantle kinematics data were subdivided into the life-history stages identified by Segawa (1987). This scheme separates *S. lessoniana* into seven size classes based on morphological and ecological characteristics. The squid used in the experiments include four of Segawa's (1987) life-history stages: hatchling (5 mm to 10 mm DML), juvenile 1 (11 mm to 25 mm DML), juvenile 2 (26 mm to 40 mm DML), and young 2 (60 mm to 100 mm DML). After subdivision into the appropriate life-history stage, the data in each stage were compared with a one-way ANOVA. Pairwise comparisons were made using the Student-Newman-Keuls method of comparison (Zar, 1996). This analysis

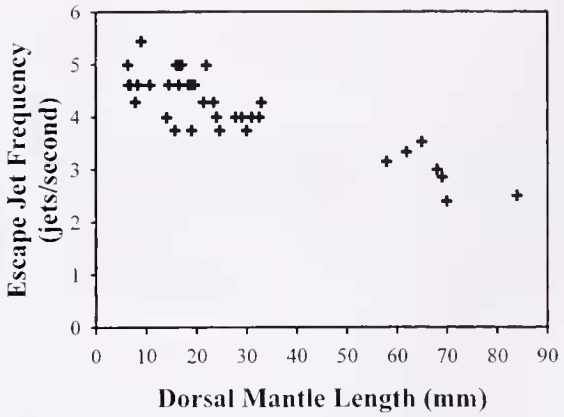

Figure 2. Ontogenetic change in escape-jet frequency. Each point represents the average frequency of at least two consecutive escape jets. Escape-jet frequency was inversely correlated with squid size (Spearman rank order correlation coefficient, -0.75, $P < 0.0001$, $n = 38$).

was appropriate because the data in each stage were distributed normally (Kolmogorov-Smirnov goodness of fit test, $P > 0.4$ for each stage; Zar, 1996).

The mantle wall thickness and mantle radius data were log transformed and regressed against dorsal mantle length using a least-squares technique (Zar, 1996). Student's t distribution was used to test the slopes against the null hypothesis slope of 1.0 (Zar, 1996).

Results

Escape-jet behavior

Tethered specimens of *Sepioteuthis lessoniana* escape jetted spontaneously upon recovery from the anesthesia and in response to visual stimuli outside the aquarium. Squid escape jetted periodically during the experimental trials and frequently jetted multiple times in succession. The number of escape jets performed consecutively seemed to vary with the size and age of the animal, with smaller, younger squid performing more consecutive escape jets than larger, older squid. Hatchling-stage squid (5 mm to 10 mm DML) often jetted five times in rapid succession, paused briefly, and then repeated the series of five jets two or three additional times. Such behavior was never observed in squid larger than about 25 mm DML (the juvenile 2 life history stage of Segawa, 1987). The escape-jet frequency of smaller, younger squid was higher than that of older and larger squid (Fig. 2; correlation coefficient, -0.75, $P < 0.0001$, $n = 38$). For example, newly hatched squid performed four to five escape-jet cycles per second, whereas two to three escape-jet cycles per second were recorded for the largest squid.

Mantle kinematics

The mantle kinematics during escape-jet behavior varied both in an individual squid over time and among all the squid studied. There were two distinct modes of mantle movement immediately prior to the start of an escape jet. In one mode, there was little mantle hyperinflation and the mantle cavity was ventilated, presumably by contraction of the circumferential musculature (Fig. 3A; see Gosline *et al.*, 1983). In the other mode, the mantle cavity was ventilated primarily by mantle hyperinflation, presumably by contraction of the radial musculature (Fig. 3B; see Gosline *et al.*, 1983). There was no correlation between squid size and the mode of mantle kinematics prior to the start of an escape jet. Many of the squid studied exhibited both modes of mantle kinematics, but the second mode (hyperinflation) was the most common.

Regardless of age or size, the escape jet was stereotyped. At the start, the mantle hyperinflated, filling the mantle cavity with water (Fig. 4A). Next, the collar flaps closed and the anteriormost edge of the mantle began to contract (analogous to a drawstring closing a bag) (Fig. 4B). The contraction of the anterior mantle edge was most noticeable in

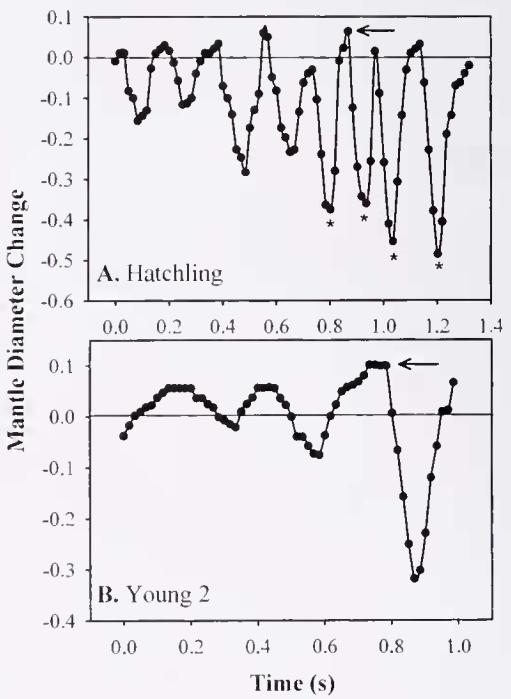

Figure 3. Mantle diameter change over time. The horizontal line at 0.0 indicates the resting mantle diameter of the anesthetized squid. The negative numbers indicate mantle contraction, and positive values denote mantle hyperinflation. (A) A hatchling stage squid (5.5 mm dorsal mantle length, DML) that performed four consecutive escape jets (indicated by asterisks). The arrow indicates a mantle hyperinflation immediately prior to an escape jet. Note that the low-amplitude mantle movements prior to the escape jets do not involve substantial mantle hyperinflation. (B) A single escape jet from a young 2 stage squid (65 mm DML). The arrow indicates the mantle hyperinflation prior to the start of the escape jet. Note that the lower amplitude mantle movements prior to the escape jet consist almost entirely of mantle hyperinflation and do not involve substantial mantle contraction.

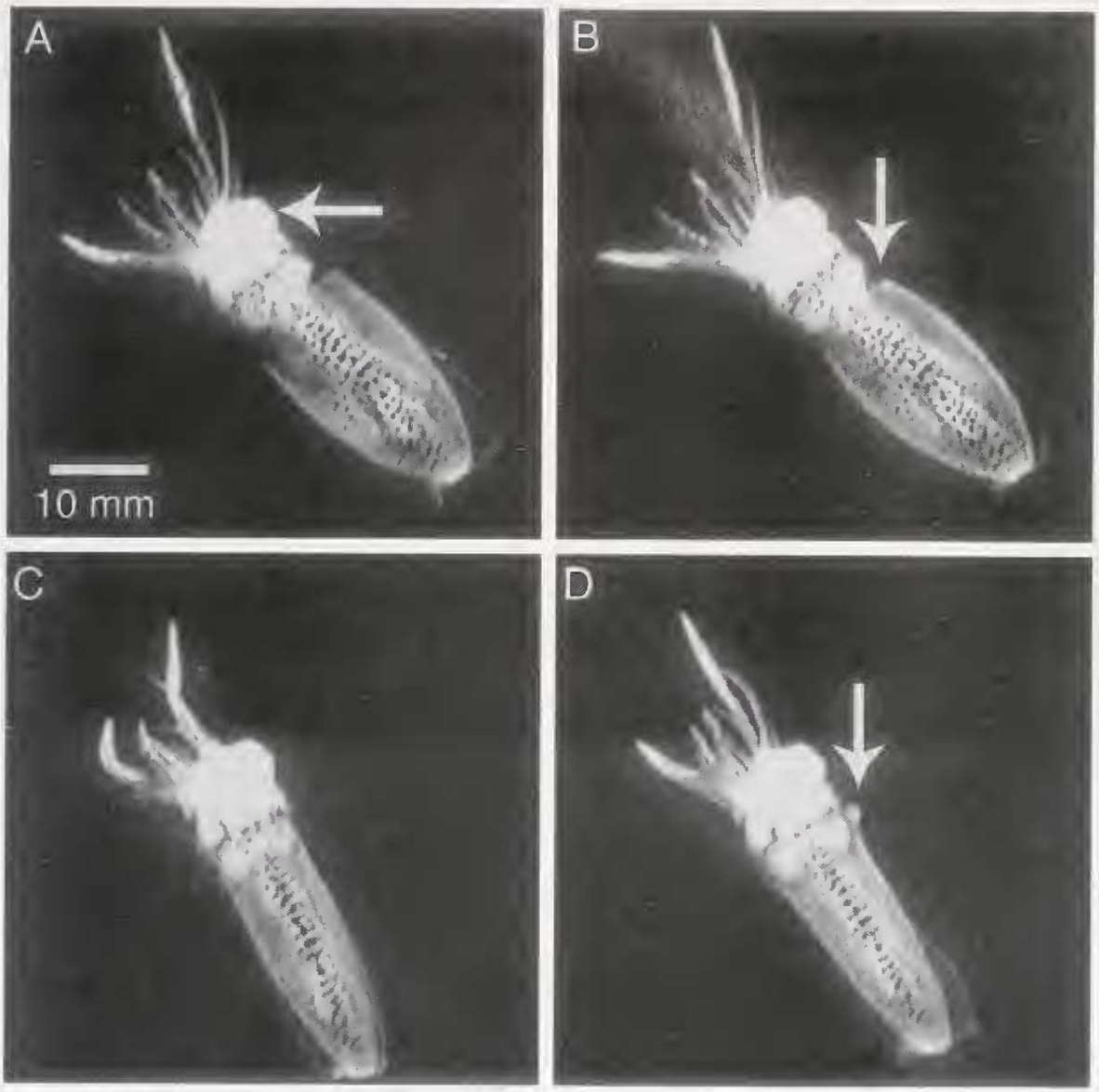

Figure 4. Nonconsecutive digitized video frames from an escape jet by a 3-week-old specimen of *Sepioteuthis lessoniana* (25-mm DML). (A) The squid immediately before the start of mantle contraction. The mantle is fully expanded, and the mantle cavity is full of water. The bright region of reflection on the head (arrow) is the plastic washer of the tethering apparatus. (B) The squid just after the start of the escape jet. The anterior edge of the mantle (arrow) has contracted, and the remainder of the mantle is just beginning to contract. (C) The mantle near its maximum contraction for the escape jet. The head is drawn back into the mantle cavity, and the fins are folded along the body. (D) The end of the exhalant phase and the start of the inhalant phase of the escape jet. The fins (barely visible on right side) are unfurling and beginning to undulate. The head is maximally withdrawn into the mantle cavity, and the anterior edge of the mantle is starting to flare (arrow) away from the head.

squid larger than 40 mm DML (about 5 to 6 weeks post hatching). One video field (about 17 ms) after the start of anterior mantle-edge contraction, two events occurred: (1) the fins were folded against the ventral side of the mantle, and (2) the remainder of the mantle began to contract rapidly, expelling water from the mantle cavity through the funnel (Figs. 4B, C). Nearly simultaneous with folding of the fins, the head was drawn back into the mantle cavity, presumably by the activation of the head retractor muscles. Maximal head retraction was completed within two video fields (about 34 ms) and was maintained until the end of the exhalant phase of the jet (Fig. 4C). At the end of the exhalant phase of the jet, the fins unfolded and began undulating immediately. Concurrent with fin unfolding, the

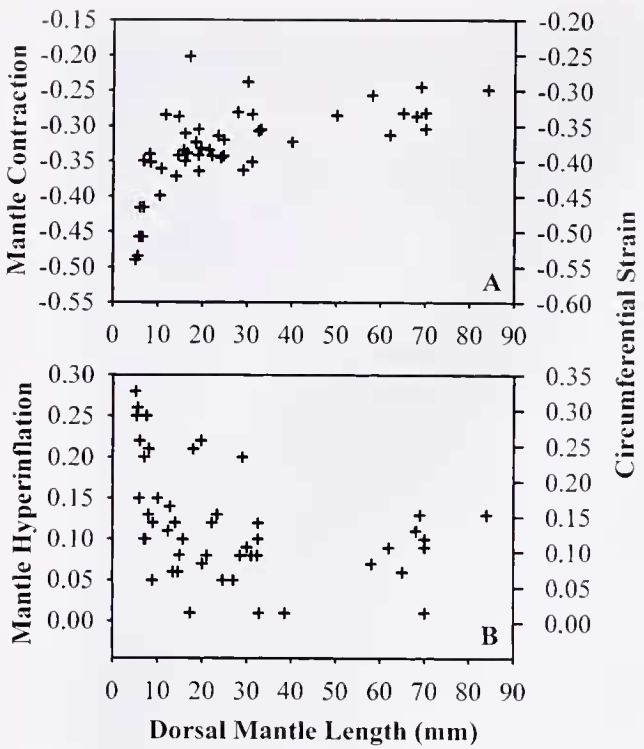

Figure 5. Ontogenetic changes in mantle contraction and mantle hyperinflation during the escape jet. Each point represents the maximum mantle diameter change (contraction or hyperinflation) for an individual squid during an escape jet. (A) Mantle contraction and circumferential strain *versus* dorsal mantle length. The plot shows a significant decrease in the maximum mantle contraction of the escape jet during ontogeny (Spearman rank order correlation coefficient, 0.70, $P < 0.0001$, $n = 55$). (B) Mantle hyperinflation prior to the start of an escape jet *versus* dorsal mantle length. The plot shows a significant ontogenetic decrease in maximum mantle hyperinflation prior to an escape jet (Spearman rank order correlation coefficient, -0.49, $P < 0.0001$, $n = 49$). For A and B, the mantle contraction and hyperinflation scales differ from the circumferential strain scales because both mantle contraction and hyperinflation are measures of the outer circumference of the mantle, whereas circumferential strain is a measure of changes in mantle wall circumference at the midpoint of the thickness of the mantle wall, and mantle thickness increases during contraction (because the mantle wall is isovolumetric).

anterior margin of the mantle flared outward (Fig. 4D). In animals smaller than 20 mm DML, this flaring was usually accompanied by even greater contraction of the mantle in the anterior ⅓ of the mantle.

Ontogeny of mantle kinematics

A significant ontogenetic change in the amplitude of mantle movement during escape-jet behavior was observed in *S. lessoniana.* In smaller and younger animals there was a greater change in mantle diameter than in larger, older squid (Fig. 5A; Spearman rank order correlation coefficient, 0.7, $P \ll 0.001$, $n = 55$). In newly hatched squid, the mantle contracted 41% to 49% during the escape jet, but it contracted by only 25% to 32% in larger animals (Fig. 5A; see Table 1 for descriptive statistics based on life history stage). After dividing the data into the life-history stages described by Segawa (1987), the average mantle contraction during the escape jet of the hatchling stage (5 mm to 10 mm DML) squid was significantly greater than in any other life history-stage measured (one-way ANOVA, Student-Newman-Keuls test, $P < 0.05$; Table 1). In addition, the average mantle contraction of squid in the juvenile 1 stage (11 mm to 25 mm DML) was significantly larger than squid in the young 2 stage (60 mm to 100 mm DML) (one-way ANOVA, Student-Newman-Keuls test, $P = 0.05$; Table 1).

There was a significant ontogenetic decrease in the amplitude of mantle hyperinflation prior to the start of the escape jet (Spearman rank order correlation coefficient, -0.49, $P \ll 0.001$, $n = 49$). In newly hatched *S. lessoniana,* the mantle hyperinflated between 15% and 27%, but it hyperinflated only 1% to 15% in older, larger animals (Fig. 5B; see Table 1 for descriptive statistics). After dividing the data into the life-history stages of Segawa (1987), the average mantle hyperinflation prior to the start of the escape jet was significantly greater in the hatchling stage squid than in all the other stages (one-

Table 1

Comparison of mantle kinematics during the escape jet among squid divided into the life-history stages defined by Segawa (1987)

Life-history stage	Maximum contraction	Maximum hyperinflation	Maximum contraction rate (lengths/s)
Hatchling	-0.40 ± 0.057 (13)	0.18 ± 0.072 (14)	8.6 ± 2.1 (14)
Juvenile 1	-0.32 ± 0.037 (23)*	0.11 ± 0.015 (15)	4.8 ± 1.2 (16)
Juvenile 2	-0.31 ± 0.040 (8)	0.086 ± 0.054 (11)	3.8 ± 1.7 (10)
Young 2	-0.28 ± 0.024 (9)*	0.088 ± 0.038 (9)	3.8 ± 0.55 (9)

Values represent mean maximum mantle contraction, mantle hyperinflation, and mantle contraction rate during the escape jet plus or minus the standard deviation of the mean. The number of squid in the sample is in parentheses. Maximum values for mantle contraction amplitude, mantle hyperinflation amplitude, or mantle contraction rate for all squid in a life-history stage were pooled to calculate the mean and the standard deviation. In each column, the mean value for the hatchling stage squid was significantly different from the mean for the juvenile 1, juvenile 2, and young 2 life-history stages (one-way ANOVA on ranks, $P < 0.05$). The asterisks in the Maximum contraction column denote a significant difference in mantle contraction between the juvenile 1 and young 2 life-history stages (one-way ANOVA on ranks, $P = 0.05$). Other within-column comparisons of mantle kinematics were not significantly different.

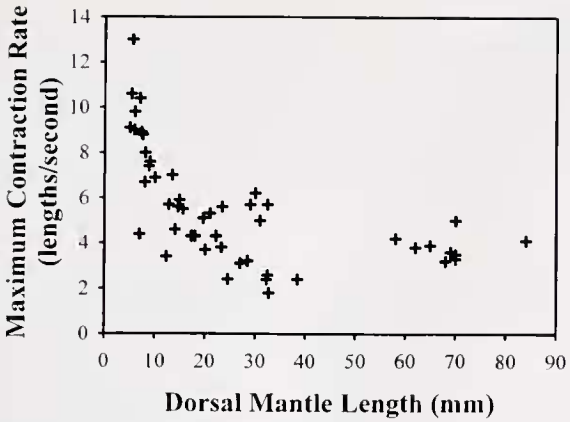

Figure 6. Ontogenetic change in the maximum rate of mantle contraction. Each point represents the maximum rate of mantle contraction during the escape jet for one individual. The maximum mantle contraction rate of the escape jet decreased significantly during ontogeny (Spearman rank order correlation coefficient, -0.76, $P < 0.0001$, $n = 49$).

way ANOVA, Student-Newman-Keuls test, $P < 0.05$; Table 1).

The maximum rate of mantle contraction during the escape jet was highest in newly hatched squid and declined during ontogeny (Fig. 6; Spearman rank order correlation coefficient, -0.76, $P \ll 0.001$, $n = 49$). The maximum rate of mantle contraction varied from 7 to 13 mantle circumference lengths per second in newly hatched squid and from 3 to 5 lengths per second in the largest squid (Fig. 6). A one-way ANOVA among the life-history stages (Segawa, 1987) indicated that hatchling stage *S. lessoniana* had a significantly greater maximum rate of mantle contraction during the escape jet than all other life history stages (Student-Newman-Keuls test, $P < 0.05$; Table 1).

Morphometrics

Mass-specific mantle cavity volume decreased during ontogeny (Fig. 7A). Despite the variation among squid of similar size, there was a significant negative correlation between mass-specific mantle cavity volume and dorsal mantle length (Spearman rank order correlation coefficient, -0.50, $P = 0.002$, $n = 36$).

The thickness of the mantle wall increased during ontogeny (Fig. 7B). The slope of the regression, 1.29, was significantly greater than 1 (Student's t test, $P < 0.01$).

Mantle radius also increased during ontogeny (Fig. 7C). The slope of the regression, 0.85, was significantly less than 1 (Student's t test, $P < 0.01$).

Discussion

The escape-jet sequence

The general pattern of the escape jet did not vary with squid age or size. However, the mantle kinematics during an escape jet did change as the squid grew. These ontogenetic changes in escape-jet kinematics may arise from alterations in the neurophysiology (Gilly *et al.*, 1991), muscle physiology (Preuss *et al.*, 1997), morphology (Moltschaniwskyj, 1995), or mechanical properties of the mantle. Furthermore, the changes may have implications

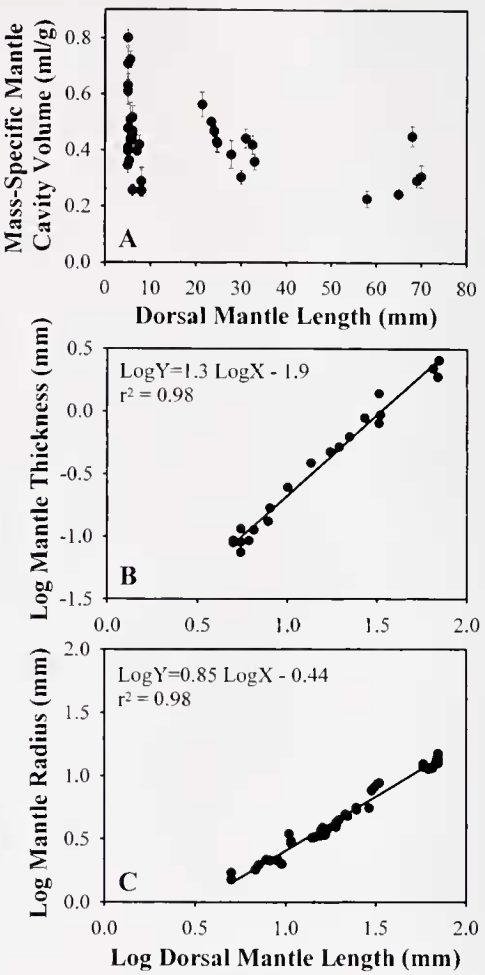

Figure 7. Ontogenetic changes in mantle morphometrics. (A) Mass-specific mantle cavity volume *versus* dorsal mantle length. Each point represents the average of between three and five measurements of mantle cavity volume for each squid ± the standard error of the mean. Dividing the average mantle cavity volume for one squid by the wet weight of the same animal normalized the data for the volume of the mantle cavity. Mass-specific mantle cavity volume decreased significantly during ontogeny (Spearman rank order correlation coefficient, -0.50, $P = 0.002$, $n = 36$). (B) Log mantle wall thickness *versus* log dorsal mantle length. The equation for the least-squares regression and the corrected r^2 value are listed at the upper left. The slope of the regression (1.29) was significantly greater than 1.0 (Student's t test, $P < 0.01$), indicating a positive allometric relationship between mantle wall thickness and mantle length. (C) Log mantle radius *versus* log dorsal mantle length. The equation for the least-squares regression and the corrected r^2 value are listed at the upper left. The slope of the regression (0.85) was significantly less than 1.0 (Student's t test, $P < 0.01$), indicating a negative allometric relationship between mantle radius and mantle length.

for the mechanics of escape-jet locomotion during growth.

Fatigue

The relative proportions of circumferential muscle fiber types in the mantle of *S. lessoniana* change during ontogeny (Thompson, 2000; Thompson and Kier, 2001). Newly hatched individuals of *S. lessoniana* have a larger proportion of mitochondria-rich circumferential muscle fibers (analogous to vertebrate red muscle fibers, see Bone *et al.*, 1981, and Mommsen *et al.*, 1981) than older, larger squid. Preuss *et al.* (1997) reported a similar change during growth in the relative proportion of circumferential muscle fiber types in the mantle of another loliginid squid, *Loligo opalescens*. Preuss *et al.* (1997) suggested that the greater proportion of mitochondria-rich circumferential mantle muscle fibers made the hatchling squid more resistant to fatigue than older, larger animals. The data from the present study support their hypothesis. Small, young specimens of *S. lessoniana* were able to perform more consecutive escape jets and seemed to tire much less readily than their larger, older counterparts. However, motivational differences between small and large squid may also affect jetting behavior.

Newly hatched squid seem to rely more heavily on frequent jet locomotion than do larger squid (Fields, 1965; Hoar *et al.*, 1994; Preuss *et al.*, 1997). Two reasons have been suggested for this tendency. First, the fins of newly hatched squid are rudimentary relative to the adult fins (Boletzky, 1974; Okutani, 1987; Hoar *et al.*, 1994), and it has been proposed that these diminutive fins may not generate sufficient thrust for locomotion or hovering (Boletzky, 1987; Hoar *et al.*, 1994). Second, most newly hatched squid live in a fluid regime that is characterized by an intermediate Reynolds number (estimated from data in Packard, 1969, and O'Dor *et al.*, 1986; see Jordan, 1992, and Daniel *et al.*, 1992, for further discussion of intermediate Re) and in which the near parity of viscous and inertial forces inhibits coasting after a jet. Unlike large squid that can perform a single jet and then coast for a considerable distance, small squid must jet continuously to locomote. Hence, there may be an advantage in having a large proportion of the locomotor musculature specialized for fatigue resistance, particularly if jetting is the primary mode of locomotion. The price for such specialization, however, may be a reduction in the peak force produced by the mantle musculature during contraction.

Mantle kinematics

The mantle cavity of a hatchling of *S. lessoniana* holds a proportionately greater volume of water than the mantle cavity of a larger squid (Fig. 7A). In addition, a larger proportion of this volume is ejected from a hatchling during an escape jet (Fig. 5A). Finally, the maximum rate of mantle contraction during an escape jet is highest in a newly hatched squid (Fig. 6). Taken together, these data imply that mass flux (*i.e.*, the product of the density of water in the mantle cavity and the volume rate of water flow out of the mantle cavity) during the escape jet is proportionately greater in hatchling than in larger, older individuals of *S. lessoniana*.

We used the mantle kinematics and morphometric data to calculate the relative mass flux during the escape jet in two life stages of *S. lessoniana:* a 5.5-mm-DML hatchling stage and a 65-mm-DML young 2 stage. We modeled the mantle as a cylinder with the "resting" wall thickness and radius calculated from the regressions of the mantle wall thickness (Fig. 7B) and mantle radius (Fig. 7C) data. To simplify the calculations, we based them on a transverse slice of the cylinder at ⅓ DML. We assumed that both the length of the cylinder and the volume of the cylinder wall were constant; thus, the cylinder-wall area of the slice was held constant during the calculations. The initial mass-specific mantle cavity volume for each squid was obtained from the data in Figure 7A. We used the data for average mantle contraction and the maximum rate of mantle contraction from Table 1 to calculate the amplitude and rate of changes in mantle radius. We used equation (2) to calculate the increase in mantle wall thickness during the simulated jet. Finally, we calculated the relative mass (*i.e.*, mass of water divided by mass of squid) of water remaining in the mantle cavity during the simulated jet at 25-ms intervals.

The calculations predict greater relative mass flux during the escape jet in the hatchling stage squid than in the young 2 stage (Fig. 8A). The average mass flux over the duration of the exhalant phase of the escape jet in a hatchling stage squid is about 2 times greater than that of an animal in the young 2 stage (Fig. 8A).

We calculated the average mass flux over the entire duration of the exhalant phase of the escape jet for the 55 squid from Figure 5A. We modeled the mantle as a cylinder of constant length with a mantle cavity volume determined from Figure 7A. Using the mantle contraction data from Figure 5A, and calculating changes in the thickness of the mantle wall during the jet using equation (2), we calculated the normalized mass of water in the mantle cavity (*i.e.*, mass of water divided by mass of squid) at the start and at the end of an escape jet. The change in normalized mass was divided by the duration of the exhalant phase of the jet to give the average mass flux. The calculations show an ontogenetic decrease in the normalized average mass flux of the escape jet (Fig. 8B). Mass flux is proportionately highest in hatchling squid and decreases rapidly during growth (Fig. 8B; correlation coefficient, -0.81, $P < 0.0001$, $n = 55$).

Does the predicted ontogenetic decline in relative mass flux imply that the mass-specific thrust produced the escape jet is highest early in ontogeny? Mass flux constitutes only

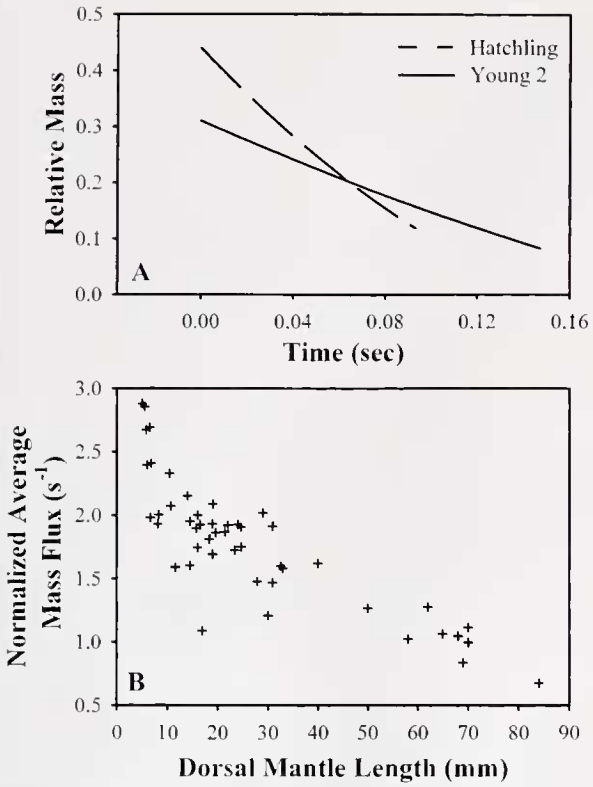

Figure 8. Ontogenetic differences in the mass flux of the escape jet. (A) Calculation of the relative mass of water remaining in the mantle cavity *versus* the time course of the exhalant phase of one escape jet. The dashed line represents a hatchling stage squid (5.5 mm dorsal mantle length) and the solid line a young 2 stage animal (65 mm dorsal mantle length). For each squid, the relative mass of water in the mantle cavity at 0.025-s intervals during the escape jet was calculated using morphometric and mantle kinematics data. See the Discussion for more details. The data for each animal were fitted with a polynomial equation. The equations are, $Y = 1.7X^2 - 1.8X + 0.31$ ($r^2 = 0.99$) for the young 2 squid and $Y = 9.3X^2 - 4.3X + 0.44$ ($r^2 = 0.99$) for the hatchling squid. The derivative of each equation yields the average mass flux during the escape jet. The average mass flux of the hatchling animal is approximately 2 times greater than that for the larger animal. Note that mass flux is highest early in the escape jet and diminishes at the end of the escape jet. (B) Calculation of the average mass flux of the escape jet *versus* dorsal mantle length. Each point represents the average mass flux of the exhalant phase of the escape jet normalized by the wet weight of the squid. Normalized average mass flux decreased significantly during ontogeny (Spearman rank order correlation coefficient, -0.81, $P < 0.0001$, $n = 55$). See the Discussion for more details.

a portion of the total jet thrust. Under steady-state conditions, the instantaneous thrust produced during a jet is proportional to the product of the instantaneous mass flux and the instantaneous velocity of the water exiting the funnel (averaged over the funnel aperture; Vogel, 1994). Because it is likely that unsteady effects are important in jet locomotion (Anderson and DeMont, 2000), an unsteady term must also be included in an equation used to calculate jet thrust (see Anderson and DeMont, 2000).

Under both steady-state and unsteady conditions, the velocity of water exiting the funnel depends, in large part, on the diameter of the funnel aperture. The funnel complex is largest in newly hatched squid and decreases in relative size during ontogeny (Boletzky, 1974; unpubl. obs. of *S. lessoniana* and *Loligo pealei*). Unfortunately, funnel aperture cannot be determined simply from the size of the funnel of an anesthetized squid because it is a muscular structure that changes shape during a single jet (Zuev, 1966; O'Dor, 1988; Anderson and DeMont, 2000). Furthermore, measuring funnel aperture accurately during escape-jet locomotion in small hatchling and juvenile squid is not currently feasible. Without data on the scaling of the funnel aperture and dynamic changes in the aperture during a jet cycle, it is not possible to make precise predictions about the mass-specific thrust produced during the escape jet.

Whether jet thrust is generated by means of steady or unsteady mechanisms, the greater relative mass flux predicted for hatchling-stage individuals of *S. lessoniana* could allow a given thrust to be achieved with a relatively low jet velocity. This may result in a hatchling stage squid having a higher propulsion efficiency than an older, larger squid. Anderson and DeMont (2000) calculated the hydrodynamic propulsion efficiency (η) of the exhalant phase of the jet stroke using the following equation of rocket motor propulsion efficiency:

$$\eta = (2VV_j)/(V^2 + V_j^2), \quad (3)$$

where V is the velocity of flow past the squid and V_j is the velocity of the jet relative to the squid. According to equation (3), the highest propulsion efficiency is achieved when V_j approximates V. Because V_j must be greater than V for a squid to accelerate, relatively lower jet velocity increases propulsion efficiency. Anderson and DeMont (2000) emphasize, however, that the overall propulsion efficiency of the jet includes both the efficiency of the jet stroke and the efficiency of refilling the mantle cavity. A thorough ontogenetic comparison of total hydrodynamic propulsion efficiency must, therefore, also consider the efficiency of mantle cavity refilling.

In the intermediate Reynolds number fluid regime of the newly hatched and juvenile squid, the generation of jet thrust may not be represented accurately by existing equations. Previous theoretical treatments consider jet propulsion at high Reynolds numbers. In the absence of a mathematical model of jet locomotion at these intermediate Reynolds numbers, measurements of the actual thrust produced are required. Therefore, direct measurements of the thrust produced during an escape jet are needed to understand how the ontogenetic changes in mantle kinematics affect thrust.

Skeletal support and mantle kinematics

In many vermiform animals, the arrangement of connective tissue fibers in the body wall helps to control the shape of the animal during locomotion and movement (*e.g.*, Harris and Crofton, 1957; Clark and Cowey, 1958). Similarly, the ontogenetic changes in mantle kinematics during escape-jet locomotion may result from ontogenetic alterations in the organization and the mechanical properties of the skeletal support system of the squid mantle.

In the mantle, skeletal support for locomotion is provided by a complex arrangement of fibers of muscle and connective tissue (Ward and Wainwright, 1972; Bone *et al.*, 1981). As described earlier, the connective tissue fibers are arranged in distinct networks: the inner tunic, the outer tunic, and three distinct systems of intramuscular (IM) fibers—IM-1, IM-2, and IM-3 (Ward and Wainwright, 1972; Bone *et al.*, 1981; for review, see Gosline and DeMont, 1985). The fibers in all the IM systems are collagenous (Ward and Wainwright, 1972; Gosline and Shadwick, 1983a; MacGillivray *et al.*, 1999), and the collagen fibers in IM-1 and IM-2 are hypothesized to antagonize the circumferential muscles that provide power for locomotion.

The organization of collagen fibers in the outer tunic and IM fiber networks of the mantle changes dramatically during the ontogeny of *S. lessoniana* (Thompson, 2000; Thompson and Kier, 2001). The IM-1 collagen fiber angle (*i.e.*, the angle of the collagen fiber relative to the long axis of the mantle) is lowest in newly hatched squid and increases exponentially during growth in squid up to 15 mm DML. In squid larger than about 15 mm DML, IM-1 fiber angle does not change substantially. IM-2 collagen fiber angle (*i.e.*, the angle of the collagen fiber relative to the outer curvature of the mantle) is lowest in hatchlings and rises exponentially until the squid reach 15 mm DML. In animals larger than 15 mm DML, IM-2 fiber angle increases only slightly with size. The correlation between these ontogenetic alterations in connective tissue organization and the mantle kinematics measured in this study is striking (Fig. 9). Maximum mantle contraction (Fig. 5A), maximum mantle hyperinflation (Fig. 5B), and maximum mantle contraction rate (Fig. 6) all change exponentially up to a dorsal mantle length of about 15 mm.

It is possible that the allometric changes in mantle thickness and mantle radius (Fig. 7B, C) might, at least in part, underlie the ontogenetic change in IM-1 and IM-2 fiber angle. We were unable, however, to detect a clear relationship between the scaling of mantle thickness or radius and IM-1 or IM-2 fiber angle.

Simple mathematical models (Thompson, 2000; Thompson and Kier, 2001) of the ontogenetic changes in IM-1 and IM-2 fiber angle predict significantly greater amplitude of mantle movements during escape-jet locomotion in newly hatched squid than in older, larger animals. The models, which consider only the fiber angle and probable mechanical properties of the IM collagen fibers (see Gosline and Shadwick, 1983b), predict that mantle circumference changes up to −45% are possible in hatchling stage squid, whereas changes of only −25% to −30% are possible in squid at the young 2 stage (Thompson, 2000; Thompson and Kier, 2001). The present study supports the predictions of the models. Maximum mantle contraction during the escape jet in hatchlings of *S. lessoniana* ranged from −41% to −49% and from −27% to −32% in animals at the young 2 stage. Additional work on the ontogeny of the mechanical properties of squid mantle collagen is necessary to understand better the relationship among connective tissue organization, mantle mechanical properties, and mantle function.

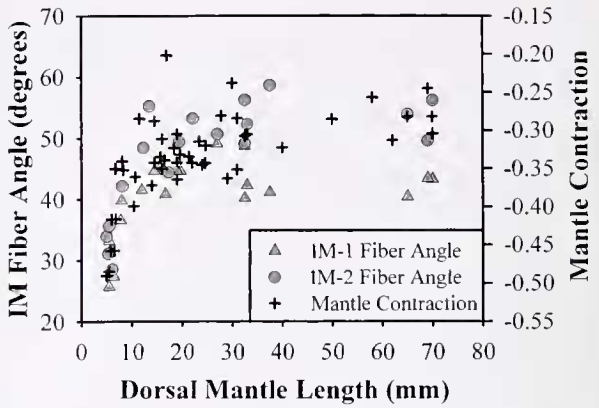

Figure 9. Correlation between ontogenetic changes in intramuscular collagen fiber angle and the mantle kinematics of the escape jet. The maximum mantle contraction during an escape jet (data from Fig. 5A) is indicated by the black crosses, and the scale is on the right side of the plot. The gray triangles indicate the average fiber angle of intramuscular fiber system 1 (IM-1) collagen fibers, and the gray circles denote the average fiber angle of IM-2 collagen fibers. Note the correlation between IM-1 and IM-2 average fiber angles and the mantle kinematics of the escape jet.

Muscle mechanics

The maximum rate of mantle contraction was significantly higher in newly hatched individuals of *S. lessoniana* than in the larger animals (Fig. 6; Table 1). The shortening velocity of muscle fibers depends on the load of the muscle, the length of the thick filaments and sarcomeres, and the rate of cross-bridge cycling (Schmidt-Nielsen, 1997). The loading of the muscle fibers during jet propulsion is difficult to measure. It should be possible, however, to measure the contractile properties and myofilament dimensions of the circumferential muscle from an ontogenetic series of squid to examine the possibility of a change in performance of the muscle during ontogeny.

Comparison of the shortening speed of the circumferential muscles calculated here for *S. lessoniana* with previous

measurements in adults of *Alloteuthis subulata* and *Sepia officinalis* are complicated by differences in temperature. The unloaded shortening speed at 11 °C of the circumferential musculature in *A. subulata* and *S. officinalis* was measured to be 2.0 lengths per second and 1.5 lengths per second, respectively (Milligan *et al.*, 1997). In *S. lessoniana*, the maximum rate of mantle contraction at 23 °C ranged from a high of 13 lengths per second in the hatchlings to 4 in the young 2 stage squid.

Although the Q_{10} for cephalopod muscles has not been measured, previous work on type 1 and type 2 iliofibularis muscle fibers from *Xenopus laevis* (Lännergren *et al.*, 1982) revealed a Q_{10} of approximately 2 over this temperature range. Thus, although the difference in measured shortening velocity between the young 2 stage of *S. lessoniana* and the adult of *A. subulata* may be due to temperature, it is unlikely that the much higher velocities measured in the hatchlings are simply an effect of temperature. In addition, the circumferential muscles are contracting against a load during an escape jet, and thus the unloaded shortening velocity of circumferential muscle in *S. lessoniana* will be higher than the values reported here.

In conclusion, we have described significant ontogenetic changes in the mantle kinematics of the escape jet in tethered squid. These kinematic changes are correlated strongly with alterations in the organization of the connective tissue fibers in the mantle; furthermore, they may affect the mass flux of the escape jet. An analysis of the mechanics of escape-jet locomotion in an ontogenetic series of squid is needed to better comprehend the implications of growth-related changes in mantle kinematics. Such an analysis will help us to understand the functional consequences of ontogenetic changes in morphology and will provide insight into the evolution of the form and function of hydrostatic skeletons.

Acknowledgments

This research was supported by NSF grants to W.M.K. (IBN-9728707 and IBN-9219495). Grants and fellowships to J.T.T. from the Wilson Fund, the American Malacological Society, and Sigma Xi helped defray research expenses. We thank L. Walsh at the NRCC for her expertise in shipping squid cross-country. We thank J. M. Gosline, S. Johnsen, J. Taylor, T. Uyeno, and two anonymous reviewers for constructive comments and suggestions on an earlier version of the paper.

Literature Cited

Anderson, E. J., and M. E. DeMont. 2000. The mechanics of locomotion in the squid *Loligo pealei*: locomotory function and unsteady hydrodynamics of the jet and intramantle pressure. *J. Exp. Biol.* **203:** 2851–2863.

Boletzky, S. v. 1974. The "larvae" of Cephalopoda: A review. *Thalassia Jugosl.* **10(1/2):** 45–76.

Boletzky, S. v. 1987. Juvenile behaviour. Pp. 45–60 in *Cephalopod Life Cycles. Vol. II: Comparative Reviews*, P. R. Boyle, ed. Academic Press, New York.

Bone, Q., A. Pulsford, and A. D. Chubb. 1981. Squid mantle muscle. *J. Mar. Biol. Assoc. UK* **61:** 327–342.

Calder, W. A. 1984. *Size, Function, and Life History.* Harvard University Press, Cambridge.

Chen, D. S., G. v. Dykhuizen, J. Hodge, and W. F. Gilly. 1996. Ontogeny of copepod predation in juvenile squid (*Loligo opalescens*). *Biol. Bull.* **190:** 69–81.

Choe, S. 1966. On the eggs, rearing, habits of the fry, and growth of some Cephalopoda. *Bull. Mar. Sci.* **16:** 330–348.

Clark, R. B., and J. B. Cowey. 1958. Factors controlling the change of shape of certain nemertean and turbellarian worms. *J. Exp. Biol.* **35:** 731–748.

Daniel, T. L., C. Jordan, and D. Grunbaum. 1992. Hydromechanics of swimming. Pp. 17–49 in *Advances in Comparative and Environmental Physiology. Vol. 11. Mechanics of Animal Locomotion*, R. M. Alexander, ed. Springer-Verlag, New York.

Fields, W. G. 1965. The structure, development, food relations, reproduction and life history of the squid *Loligo opalescens* Berry. *Fish Bull.* **131:** 1–108.

Gilly, W. F., B. Hopkins, and G. O. Mackie. 1991. Development of giant motor axons and neural control of escape responses in squid embryos and hatchlings. *Biol. Bull.* **180:** 209–220.

Gosline, J. M., and M. E. DeMont. 1985. Jet-propelled swimming in squids. *Sci. Am.* **252(1):** 96–103.

Gosline, J. M., and R. E. Shadwick. 1983a. The role of elastic energy storage mechanisms in swimming: an analysis of mantle elasticity in escape jetting in the squid, *Loligo opalescens*. *Can. J. Zool.* **61:** 1421–1431.

Gosline, J. M., and R. E. Shadwick. 1983b. Molluscan collagen and its mechanical organization in squid mantle. Pp. 371–398 in *The Mollusca. Vol. I: Metabolic Biochemistry and Molecular Biomechanics*, P. W. Hochachka, ed. Academic Press, New York.

Gosline, J. M., J. D. Steeves, A. D. Harman, and M. E. DeMont. 1983. Patterns of circular and radial mantle muscle activity in respiration and jetting of the squid *Loligo opalescens*. *J. Exp. Biol.* **104:** 97–109.

Hanlon, R. T., J. W. Forsythe, and S. v. Boletzky. 1985. Field and laboratory behavior of "Macrotritopus larvae" reared to *Octopus defilippi* Verany, 1851 (Mollusca: Cephalopoda). *Vie Milieu* **35(3/4):** 237–242.

Harris, J. E., and H. D. Crofton. 1957. Structure and function in the nematodes: internal pressure and cuticular structure in *Ascaris*. *J. Exp. Biol.* **34:** 116–130.

Hoar, J. A., E. Sim, D. M. Webber, and R. K. O'Dor. 1994. The role of fins in the competition between squid and fish. Pp. 27–43 in *Mechanics and Physiology of Animal Swimming*, L. Maddock, Q. Bone, and J. M. Rayner, eds. Cambridge University Press, Cambridge.

Jordan, C. E. 1992. A model of rapid-start swimming at intermediate Reynolds number: undulatory locomotion in the chaetognath *Sagitta elegans*. *J. Exp. Biol.* **163:** 119–137.

Kier, W. M. 1996. Muscle development in squid: ultrastructural differentiation of a specialized muscle fiber type. *J. Morphol.* **229:** 271–288.

Lännergren, J., P. Lindblom, and B. Johansson. 1982. Contractile properties of two varieties of twitch fibres in *Xenopus laevis*. *Acta Physiol. Scand.* **114:** 523–535.

Lee, P. G., P. E. Turk, W. T. Yang, and R. T. Hanlon. 1994. Biological characteristics and biomedical applications of the squid *Sepioteuthis lessoniana* cultured through multiple generations. *Biol. Bull.* **186:** 328–341.

MacGillivray, P. S., E. J. Anderson, G. M. Wright, and M. E. DeMont. 1999. Structure and mechanics of the squid mantle. *J. Exp. Biol.* **202:** 683–695.

Marliave, J. B. 1980. Neustonic feeding in early larvae of *Octopus dofleini* (Wülker). *Veliger* **23(4):** 350–351.

Messenger, J. B., M. Nixon, and K. P. Ryan. 1985. Magnesium chloride as an anaesthetic for cephalopods. *Comp. Biochem. Physiol.* **82C:** 203–205.

Milligan, B. J., N. A. Curtin, and Q. Bone. 1997. Contractile properties of obliquely striated muscle from the mantle of squid (*Alloteuthis subulata*) and cuttlefish (*Sepia officinalis*). *J. Exp. Biol.* **200:** 2425–2436.

Moltschaniwskyj, N. A. 1995. Changes in shape associated with growth in the loliginid squid *Photololigo* sp.: a morphometric approach. *Can. J. Zool.* **73:** 1335–1343.

Mommsen, T. P., J. Ballantyne, D. MacDonald, J. Gosline, and P. W. Hochachka. 1981. Analogues of red and white muscle in squid mantle. *Proc. Nat. Acad. Sci. USA* **78:** 3274–3278.

Moynihan, M., and A. E. Rodaniche. 1982. The behavior and natural history of the Caribbean reef squid *Sepioteuthis sepioidea*. *Fortschr. Verhaltensforsch.* Supplement 25. Verlag-Parey, Berlin. 151 pp.

O'Dor, R. K. 1988. The forces acting on swimming squid. *J. Exp. Biol.* **137:** 421–442.

O'Dor, R. K., P. Helm, and N. Balch. 1985. Can rhyncoteuthions suspension feed? (Mollusca: Cephalopoda). *Vie Milieu* **35(3/4):** 267–271.

O'Dor, R. K., E. A. Foy, P. L. Helm, and N. Balch. 1986. The locomotion and energetics of hatchling squid, *Illex illecebrosus*. *Am. Malac. Bull.* **4(1):** 55–60.

Okutani, T. 1987. Juvenile morphology. Pp. 33–44 in *Cephalopod Life Cycles, Vol. II: Comparative Reviews*, P. R. Boyle, ed. Academic Press, New York.

Packard, A. 1969. Jet propulsion and the giant fibre response of *Loligo*. *Nature* **221:** 875–877.

Prenss, T., Z. N. Lebaric, and W. F. Gilly. 1997. Post-hatching development of circular mantle muscles in the squid *Loligo opalescens*. *Biol. Bull.* **192:** 375–387.

Schmidt-Nielsen, K. 1997. *Animal Physiology*, 5th ed. Cambridge University Press, Cambridge.

Segawa, S. 1987. Life history of the oval squid, *Sepioteuthis lessoniana* in Kominato and adjacent waters central Honshu, Japan. *J. Tokyo Univ. Fish.* **74(2):** 67–105.

Shadwick, R. E., and J. M. Gosline. 1985. The role of collagen in the mechanical design of squid mantle. Pp. 299–304 in *Biology of Invertebrate and Lower Vertebrate Collagens*, A. Bairati and R. Garrone, eds. Plenum Press, New York.

Sokal, R. R., and F. J. Rohlf. 1981. *Biometry*. 2nd ed. W. H. Freeman, New York.

Stearns, S. C. 1992. *The Evolution of Life Histories*. Oxford University Press, Oxford.

Sweeney, M. J., C. F. E. Roper, K. M. Mangold, M. R. Clarke, and S. v. Boletzky (eds.). 1992. *Larval and Juvenile Cephalopods: A Manual For Their Identification. Smithsonian Contributions to Zoology*, No. 513.

Thompson, J. T. 2000. The ontogeny of mantle structure and function in the oval squid, *Sepioteuthis lessoniana* (Cephalopoda: Loliginidae). Ph.D. dissertation, University of North Carolina at Chapel Hill.

Thompson, J. T., and W. M. Kier. 2001. Ontogenetic changes in fibrous connective tissue organization in the oval squid, *Sepioteuthis lessoniana* Lesson, 1830. *Biol. Bull.* **201:** 136–153.

Villanueva, R., C. Nozais, and S. v. Boletzky. 1995. The planktonic life of octopuses. *Nature* **377:** 107.

Vogel, S. 1994. *Life in Moving Fluids*. 2nd ed. Princeton University Press, Princeton.

Ward, D. V., and S. A. Wainwright. 1972. Locomotory aspects of squid mantle structure. *J. Zool. (Lond.)* **167:** 437–449.

Werner, E. E. 1988. Size, scaling, and the evolution of complex life cycles. Pp. 60–81 in *Size-Structured Populations*, B. Ebenman and L. Persson, eds. Springer-Verlag, New York.

Zar, J. H. 1996. *Biostatistical Analysis*. Prentice Hall, Upper Saddle River, NJ.

Znev, G. V. 1966. Characteristic features of the structure of cephalopod molluscs associated with controlled movements. Ekologo-Morfologicheskie Issledovaniya Nektonnykh Zhivotnykh. Kiev, Special Publication. (Canadian Fisheries and Marine Services Translation Series 1011, 1968).